

# Yttria–Alumina–Silica Glasses with Addition of Zirconia

P. Vomacka & O. Babushkin

Department of Engineering Materials, Luleå University of Technology, S-951 87 Luleå, Sweden

(Received 25 May 1994; revised version received 18 February 1995; accepted 29 February 1995)

## Abstract

*ZrO<sub>2</sub>-free glasses and glasses containing ZrO<sub>2</sub> in the system Y<sub>2</sub>O<sub>3</sub>–Al<sub>2</sub>O<sub>3</sub>–SiO<sub>2</sub> have been investigated. Properties of compositions fired in nitrogen at 1600, 1650 and 1700°C have been assessed. The solubility limit of ZrO<sub>2</sub> in yttrium aluminosilicate liquids with a high content of Y<sub>2</sub>O<sub>3</sub> at 1700°C was determined to be 6 wt%. The hardness and density of the ZrO<sub>2</sub>-containing glasses were slightly increased compared to the ZrO<sub>2</sub>-free glass; γ-Y<sub>2</sub>Si<sub>2</sub>O<sub>7</sub> (at temperatures <1300°C) and β-Y<sub>2</sub>Si<sub>2</sub>O<sub>7</sub> (at temperatures >1300°C) monoclinic phases are the main products formed during the crystallization. An unidentified intermediate phase rich in Y, Al and Si was observed to undergo a transformation at temperatures ≥1200°C resulting in the formation of the β-Y<sub>2</sub>Si<sub>2</sub>O<sub>7</sub> phase.*

## 1 Introduction

Silicon nitride and sialon ceramics are among the most promising materials for use in structural applications at high temperatures due to their outstanding combination of mechanical, chemical and thermal properties. Processing of these materials to near-theoretical density requires the use of sintering aids to provide a medium for liquid-phase sintering since the low self-diffusivity of Si<sub>3</sub>N<sub>4</sub> does not allow densification by solid-state sintering.<sup>1</sup> Among the many oxides studied, Y<sub>2</sub>O<sub>3</sub> is one of the most useful as a sintering additive, both in terms of the refractory nature of the resulting microstructures and in terms of its oxidation resistance. Alumina is often added to enhance sinterability. On cooling, these two oxides, together with SiO<sub>2</sub>, appearing naturally on the surface of all silicon nitride powders, form a glass.<sup>2</sup> The softening of this glassy phase at high temperatures reduces mechanical strength and the upper-use temperature.

Two possible approaches to eliminate the glassy phase from the final microstructure are: (i) heat treatment to promote crystallization of the amorphous phases and (ii) alteration of the glass composition to increase the ease of crystallization.<sup>3</sup> Two-stage heat treatment, using the temperature of maximum nucleation rate for the first stage, followed by a higher annealing temperature to induce growth, has been suggested.<sup>2</sup> Other parameters also affect crystallization in the intergranular regions of Si<sub>3</sub>N<sub>4</sub> ceramics such as the thickness of these regions. While crystallization of the secondary-phase pockets is possible in most systems, glassy material always remains at the grain boundaries with only the exception of special boundaries.<sup>4</sup> Clarke<sup>5</sup> proposed that an equilibrium intergranular film thickness exists for each material composition.

The amorphous grain-boundary phase composition in Si<sub>3</sub>N<sub>4</sub> containing yttria and alumina as sintering additives can be simulated by glasses in the Y<sub>2</sub>O<sub>3</sub>–Al<sub>2</sub>O<sub>3</sub>–SiO<sub>2</sub> system. The first major study of the Y<sub>2</sub>O<sub>3</sub>–Al<sub>2</sub>O<sub>3</sub>–SiO<sub>2</sub> system was reported by Bondar and Galakov,<sup>6</sup> who developed a phase diagram in 1964. Recently Arita *et al.*<sup>2</sup> reviewed the crystallization studies in yttria–alumina–silica glasses. Several investigations have been carried out on other properties of yttria–alumina–silica glasses.<sup>7–15</sup> It was found that the density, refractive index, microhardness and thermal expansion of these glasses vary significantly with the Y<sub>2</sub>O<sub>3</sub> content. The yttria–alumina–silica glasses have high thermal expansion considering their high  $T_g$ . The high microhardness indicates good abrasion resistance. The chemical durability in distilled water is very high.

Typical glass compositions for sialons are in the ternary eutectic ‘trough’ of the Y<sub>2</sub>O<sub>3</sub>–Al<sub>2</sub>O<sub>3</sub>–SiO<sub>2</sub> system with nitrogen solubility and stable glass-forming ability extending to between 20 and 30 eq.%.<sup>16</sup> The amorphous grain-boundary phase composition in Y-sialon materials can be simulated

by oxynitride glasses in which nitrogen is substituted for oxygen in the  $Y_2O_3$ - $Al_2O_3$ - $SiO_2$  system to produce a more tightly linked glass network. It has been shown that the glassy phase in  $\beta$ -sialon material, with additions of yttria, can be crystallized to yttrium aluminum garnet—YAG—by a post-sintering heat treatment. The YAG crystallization requires either simultaneous  $Si_2N_2O$  formation or accommodation of excess Si and N within  $\beta$ -sialon.<sup>17</sup> Crystallization behaviour in oxynitride glasses has been investigated by several researchers. Leng-Ward and Lewis<sup>7</sup> studied glasses having compositions with a constant Y:Si:Al ratio of 1.04:1.27:1.27 with nitrogen contents ranging from 0 to 30 eq.% and reported the replacement of the yttrium disilicate ( $Y_2Si_2O_7$ ) by yttrium aluminum garnet with increasing nitrogen content at 1250°C for 40 h when nitrogen was mainly incorporated into  $Si_2N_2O$ . Annealing of the nitrogen glasses at 1100°C produced partial crystallization involving an intermediate phase related to nitrogen-wollastonite ( $Y_2Si_2O_4N_2$ ). Loehman<sup>14</sup> investigated glasses lying on the  $Y_2O_3$ - $SiO_2$ -AlN plane of the Y-Si-Al-O-N system and found a general trend to formation of  $Y_2Si_2O_7$  as the predominant crystalline phase at 1000, 1100 and 1200°C and longer times. Five intermediate phases (yttrium silicates, yttrium aluminum silicates or nitrogen apatite —  $Y_4Si_4O_{11}N_2$ ) were also observed. Dinger *et al.*<sup>18</sup> studied crystallization of a glass having a composition of  $Y_{0.26}Si_{0.30}Al_{0.11}ON_{0.11}$  with the crystallization proceeding by a heterogeneous nucleation mechanism, with intermetallic iron silicides acting as nuclei for the columnar dendritic  $\gamma$ - $Y_2Si_2O_7$  species. After secondary crystallization of  $YSi_2AlO_4N_2$  in interdendritic regions at 1200°C, the high-temperature polymorph of  $Y_2Si_2O_7$  ( $\delta_2$ - $Y_2Si_2O_7$ ) formed and became the predominant crystalline phase in glass crystallized at 1300°C and 1400°C. Besson *et al.*,<sup>19</sup> investigating a glass with a similar composition to that of Dinger *et al.*<sup>18</sup> containing 17 eq.% of nitrogen, observed  $Y_2Si_2O_7$  in the  $\alpha$  form below 1200°C and the  $\beta$  form above this temperature. Crystallization of the YAG phase at 1100°C and  $AlYO_3$  with  $Si_2N_2O$  at 1250°C and 1300°C was also observed. O'Meara and Dunlop<sup>20</sup> studied crystallization of glass with the composition 53 wt%  $Y_2O_3$ , 17 wt%  $Al_2O_3$  and 30 wt%  $SiO_2$  with additions of 8–15 wt%  $Si_3N_4$  at 1200°C for 12 h and found  $Y_2Si_2O_7$  ( $\alpha$ ,  $\beta$ )  $Si_2N_2O$  and YAG.

Since nucleation and growth of secondary crystalline phases are unlikely processes in grain boundaries or pockets in  $Si_3N_4$ -based ceramics, the full crystallization of the glassy phase in these materials may be difficult. Complete elimination

of this glassy phase might be achieved by another mechanism, namely the remaining intergranular phase may form a crystalline solid solution phase. Zirconia provides a good example of this behaviour since its structure can accept considerable amounts of oxides in solid solution. The microstructure of sintered  $Si_3N_4$ - $ZrO_2$ ( $Y_2O_3$ ) ceramics contains extremely small amounts of intergranular phase.<sup>21–25</sup>

Zhao *et al.*<sup>26</sup> found that addition of  $ZrO_2$  to yttria–alumina–silica glasses as a nucleating agent could shorten the incubation period of nucleation and increase the rate of nucleation. Crystallization studies reported by Drummond<sup>3</sup> on three different systems showed that the addition of nucleating agents can result in crystallization of the intergranular phases.

The present study attempts to simulate the intergranular phase in silicon nitride-based ceramics by an yttria–alumina–silica glass with an addition of zirconia. First, three  $ZrO_2$ -free powder mixtures were fired at different temperatures to assess their glass-forming tendency on furnace cooling and the obtained glasses were characterized. Following this, the solubility limit of  $ZrO_2$  in a chosen composition at 1700°C was determined by producing a series of glasses with between 0 and 11 wt%  $ZrO_2$ . These  $ZrO_2$ -containing glasses were characterized. The crystallization behaviour at different temperatures of an appropriate glass with the addition of 6 wt% zirconia was studied.

## 2 Experimental Procedure

### 2.1 Sample preparation

The experimental conditions and the composition of all the samples are given in Table 1.

Three powder mixtures in the  $Y_2O_3$ - $Al_2O_3$ - $SiO_2$  system located as indicated in Fig. 1 were fired at 1600, 1650 and 1700°C to determine the glass-forming tendency on furnace cooling (compositions 1A–3C). Samples were prepared from high-purity  $Y_2O_3$ ,  $Al_2O_3$  and  $SiO_2$  powders (Rhône Poulenc, Alcoa Chemicals, and Johnson Matthey Alfa Products, respectively). The powders were weighed in a precision balance, dry-mixed in polyethylene containers on a Siemens roller mill for 10 h and sieved. Batches of approximately 20 g each were then mechanically compacted into molybdenum crucibles and fired in a nitrogen atmosphere (pressure 0.17 MPa) at temperatures of 1600, 1650 and 1700°C for 3 h. The heating rate up to the firing temperatures was 5°C/min, the cooling rate from the firing temperatures to 1400°C was 20°C/min, from 1400–950°C, 15°C/min and from 950 to 500°C, 10°C/min. The

**Table 1.** Composition and experimental condition of the studied glasses

No.	Composition (wt%)					Experimental conditions		
	$Y_2O_3$	$Al_2O_3$	$SiO_2$	$Si_3N_4$	$ZrO_2$	Firing temp. ( $^{\circ}C$ )	Fired in	Phases after cooling from firing temp.
1A	55.3	16	28.8			1600	Nitrogen	$Y_{4.67}(SiO_4)_3O$ $Al_5Y_3O_{12}$ $AlYO_3$ amorphous
1B	55.3	16	28.8			1650	Nitrogen	$Y_{4.67}(SiO_4)_3O$ $Y_2Si_2O_7$ amorphous
1C	55.3	16	28.8			1700	Nitrogen	$Y_{4.67}(SiO_4)_3O$ amorphous
2A	51.4	19.9	28.8			1600	Nitrogen	$Al_5Y_3O_{12}$ $Y_2SiO_5$ $Y_2Si_2O_7$ amorphous
2B	51.4	19.9	28.8			1650	Nitrogen	$Y_{4.67}(SiO_4)_3O$ $Y_2Si_2O_7$ amorphous
2C	51.4	19.9	28.8			1700	Nitrogen	$Y_2Si_2O_7$ amorphous
3A	46.9	24.3	28.8			1600	Nitrogen	$Al_5Y_3O_{12}$ $Y_2Si_2O_7$ amorphous
3B	46.9	24.3	28.8			1650	Nitrogen	Amorphous
3C	46.9	24.3	28.8			1700	Nitrogen	Amorphous
4	43.1	22.4	26.5	8		1650	Nitrogen	Amorphous
5	46.9	24.3	28.8			1600	Air	Amorphous
6	46	23.8	28.2		2	1700	Nitrogen	Amorphous
7	44.6	23.1	27.3		5	1700	Nitrogen	Amorphous
8	44.1	22.8	27.1		6	1700	Nitrogen	Amorphous
9	43.7	22.5	26.8		7	1700	Nitrogen	$Y_{0.15}Zr_{0.85}O_{1.9}$ amorphous
10	43.1	22.4	26.5		8	1700	Nitrogen	$Y_{0.15}Zr_{0.85}O_{1.9}$ amorphous
11	42.7	22.1	26.2		9	1700	Nitrogen	$Y_{0.15}Zr_{0.85}O_{1.9}$ amorphous
12	42.2	21.9	25.9		10	1700	Nitrogen	$Y_{0.15}Zr_{0.85}O_{1.9}$ amorphous
13	41.7	21.6	25.6		11	1700	Nitrogen	$Y_{0.15}Zr_{0.85}O_{1.9}$ amorphous

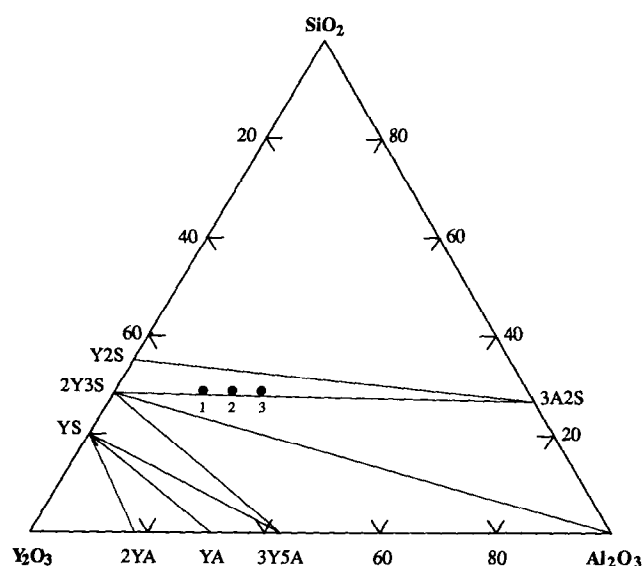


**Fig. 1.** The  $Al_2O_3$ – $Y_2O_3$ – $SiO_2$  subsolidus phase diagram<sup>6</sup> with the powder mixtures (1, 2, 3) (YS =  $Y_2O_3 \cdot SiO_2$ ; Y2S =  $Y_2O_3 \cdot 2SiO_2$ ; 2Y3S =  $2Y_2O_3 \cdot 3SiO_2$ ; YA =  $Y_2O_3 \cdot Al_2O_3$ ; 2YA =  $2Y_2O_3 \cdot Al_2O_3$ ; 3Y5A =  $3Y_2O_3 \cdot 5Al_2O_3$ ; 3A2S =  $3Al_2O_3 \cdot 2SiO_2$ ).

cooling rate was the natural cooling rate of the furnace (cold wall vacuum/pressure furnace with a graphite heater) after it has been switched off. No mass changes were observed.

A glass with composition 4, i.e. with the addition of 8 wt%  $Si_3N_4$  (KemaNord Industriekemi) was prepared at 1650°C using the same procedures as described above; this was used for comparison of the hardnesses of the produced glasses. Glass with composition 5 was prepared in air, also for comparison when subsequently characterizing glasses made in nitrogen. A batch of 20 g was fired in an alumina crucible at 1600°C for 1 h using a rapid high-temperature furnace (maximum temperature of 1600°C).

To evaluate the solubility of zirconia in the yttrium aluminosilicate liquid at 1700°C, increasing amounts of unstabilized zirconia powder (Sigma Chemical) were added to composition 3C to give compositions 6–13 of the type  $xZrO_2 + (100-x)$  (46.9  $Y_2O_3 \cdot 24.3 Al_2O_3 \cdot 28.8 SiO_2$ ) where  $x$  (in

wt%) varied between 0 and 11. The above mixing and firing procedures were used with batches of approximately 10 g each. The firing temperature was 1700°C.

A large 100g batch of composition 8 with 6 wt% of zirconia was also fired applying the same procedures. This glass was used to investigate crystallization of an yttria–alumina–silica glass containing zirconia. To improve the mixing efficiency of such a large batch, propanol was used as the mixing medium.

## 2.2 Glass characterization

Powder X-ray diffraction (Phillips X-ray diffractometer,  $\text{CuK}\alpha$  radiation) was performed on the furnace-cooled specimens to check for crystallization during cooling, to determine the solubility limit of zirconia and to identify crystalline phases in zirconia-containing glass-ceramics after the heat treatment. The lower limit of detectability of the technique lies around 2–5 wt% of a given phase. Differential thermal analysis (DTA) was carried out in a nitrogen atmosphere using an  $\text{Al}_2\text{O}_3$  powder reference standard and a heating rate 10°C/min. The infrared spectra (IR) were measured using a Perkin-Elmer 1760 X Fourier transform spectrometer equipped with a triglycine sulphate (TGS) detector. The measurements were carried out on discs pressed from powdered samples mixed with KBr. A microhardness tester with a diamond indenter was used to measure Vickers hardness. A load of 200 g was applied for 15 s on the sample whose surface had been polished with a 3- $\mu\text{m}$  spray diamond. At least 10 indentations were made on each sample, the hardness being calculated on the basis of the average length of the indentation diagonals. The density was measured with Archimedes' method, using water as the suspending medium. SEM investigations were carried out using a CamScan S4-80DV electron microscope. The nitrogen contents of the glasses were determined on powdered samples using commercially available equipment, the Leco nitrogen determinator TN-414.

## 2.3 Crystallization of an Yttria–Alumina–Silica glass containing zirconia

The investigation was carried out on glass composition 8 with 6 wt% of zirconia using an alumina tube furnace with flowing nitrogen. Pieces of approximately 1 g ( $7 \times 7 \times 4$  mm) were placed in a  $\text{Si}_3\text{N}_4$  powder bed in alumina–silica boats and heat-treated at 50°C intervals between 950 and 1400°C for 1 h with a heating rate of 250°C/h. After the heat treatment, the samples were

**Table 2.** Glass transition temperatures for compositions 3B and 3C from DTA analysis

Composition	Firing temp. (°C)	$T_g$ (°C)
3B	1650	900
3C	1700	920

removed from the high-temperature zone and cooled rapidly to room temperature in the cold zone, while still in the nitrogen atmosphere.

## 3 Results and Discussion

### 3.1 Yttria–alumina–silica glasses

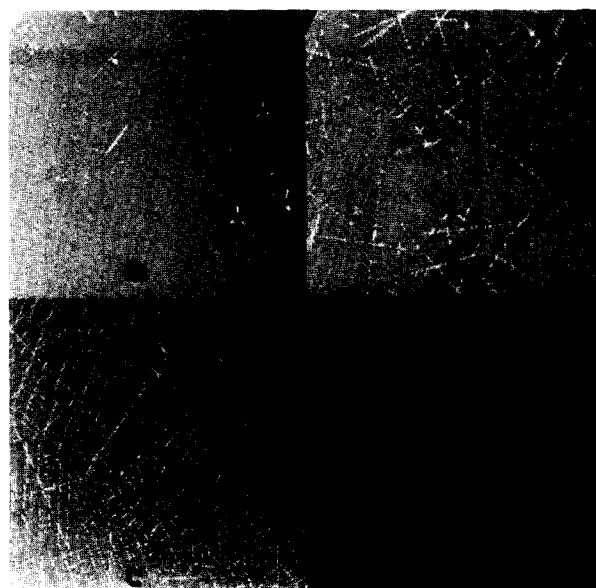
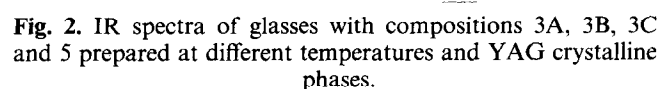
Table 1 summarizes the results of phase identification of samples furnace-cooled after firing. Only compositions 3B and 3C fired at 1650 and 1700°C gave fully amorphous material (transparent grey-coloured glasses). According to the equilibrium phase diagram,<sup>6</sup> phases expected after cooling from the firing temperatures were yttrium oxide silicates ( $\text{Y2S} = \text{Y}_2\text{O}_3 \cdot 2\text{SiO}_2$  and  $2\text{Y3S} = 2\text{Y}_2\text{O}_3 \cdot 3\text{SiO}_2$ ) and mullite ( $3\text{A2S} = 3\text{Al}_2\text{O}_3 \cdot 2\text{SiO}_2$ ). With the exception of Y2S, these phases were not found after the furnace cooling, probably because the cooling conditions were far from equilibrium; it should also be noted that the existence of the 2Y3S phase has not been confirmed and has been questioned.<sup>8,10</sup> In some cases another yttrium oxide silicate phase ( $\text{Y}_{4.67}[\text{SiO}_4]_3\text{O}$ —JCPDS: 30-1457) was identified instead.

Results from DTA analysis of glasses 3B and 3C are shown in Table 2 and indicate a shift in glass transition temperature. Loehman<sup>13–15</sup> and Ding *et al.*<sup>27</sup> have reported a similar shift of  $T_g$  to a higher temperature with increasing nitrogen content.

Hardness of glass can also be an indicator of composition changes. For example, Makishima *et al.*<sup>11</sup> compared the Vickers hardness (200 g, 15 s) of an optical glass containing PbO (4.6 GPa) with an yttria–alumina–silica glass (8.2 GPa). It was found by Hyatt and Day<sup>9</sup> that glasses of high  $\text{Y}_2\text{O}_3$  content were harder. As shown by Loehman,<sup>13–15</sup> increasing the nitrogen content increases the hardness of the yttria–alumina–silica glasses due to the nitrogen substitution for oxygen in the network to produce a more highly cross-linked structure. Here, the hardnesses of four glasses with the compositions 3B, 3C, 4 and 5 fired under different conditions were examined (Table 3). As expected, the lowest value of Vickers hardness was found for the glass fired in air and the highest for the glass prepared in nitrogen with the addition of  $\text{Si}_3\text{N}_4$  and containing 1 wt% of nitrogen. Glasses fired in 1650 ( $\leq 0.1$  wt% of

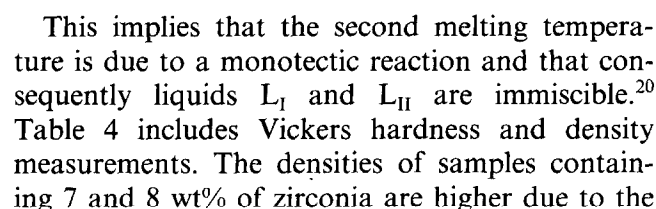
<i>Composition</i>	<i>Firing temp.</i> (°C)	<i>VH</i> (GPa)	<i>Density</i> (g cm <sup>3</sup> )	<i>Fired in</i>
3B	1650	7.69 ± 0.24	3.59	Nitrogen
3C	1700	7.96 ± 0.46	3.63	Nitrogen
5	1600	7.06 ± 0.32	3.54	Air
4	1650	9.22 ± 0.11	3.84	Nitrogen

The infrared spectra (Fig. 2) of glasses with compositions 3A, 3B, 3C and 5 revealed their structure to be a continuous, closed network. The spectrum of the sample melted at 1600°C (3A) is characterized by the presence of two absorption bands located at 920 and 1100  $\text{cm}^{-1}$ . They are associated with the cooperative antisymmetric stretching motion of silica tetrahedra containing bridging Si-O-Si and non-bridging Si-O<sup>-</sup> oxygen bonds.<sup>28</sup> The number and sequence of another group of absorption bands (770, 715, 680, 580 and 535  $\text{cm}^{-1}$ ) can be related to the YAG phase sintered as a standard at 1600°C in air. The spectra of glasses melted at 1650 and 1700°C (3B and 3C, respectively) are characterized by a broad absorption band at 890  $\text{cm}^{-1}$ . This broad band is a result of stretching modes of both the Si-O-Si and the Si-O-Al(Y) bonds. These two spectra are very similar to the spectrum of glass melted in air (5). The small shift of this band at 1700°C to 870  $\text{cm}^{-1}$  might be related to the contribution of the Si-N bonds,<sup>27,29</sup> but in view of the chemical analysis of the glasses, this contribution to the IR spectrum is



probably negligible. However, in general the location of the bond absorption at 870 and 890  $\text{cm}^{-1}$  is determined by a strong contribution of Si-O-Al(Y) stretching.

Results from DTA analysis are shown in Fig. 4. When evaluating the glass transition temperature ( $T_g$ ) of the  $ZrO_2$ -containing glasses, no significant peak above background could be identified on the DTA charts but two endotherms were recorded at 1410 and 1425°C. No mass change occurred in association with the endotherms and therefore they were interpreted as representing melting reactions. The eutectic temperature of the base mixture of oxides without zirconia has been determined as 1430°C (Fig. 4). The lowest endotherm indicates that this eutectic is lowered to 1410°C by the addition of zirconia. The melting process is assumed to proceed as follows:



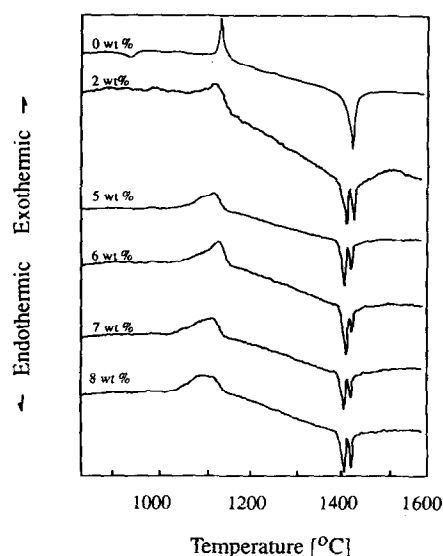


Fig. 4. DTA curves of glasses prepared at 1700°C with different  $\text{ZrO}_2$ -content.

higher density of the dendritic crystalline phase ( $5.959 \text{ g/cm}^3$ ).

### 3.3 Crystallization of a zirconia-containing glass

Composition 8 with the addition of 6 wt% of zirconia was subjected to heat treatments described in Section 2 in order to investigate the behaviour of  $\text{ZrO}_2$  in the glass.

Samples treated at 950 and 1000°C still remained as clear transparent glasses. A sample treated at 1050°C was opaque but no traces of crystalline phases could be detected in its X-ray pattern. Heat treatments at higher temperatures resulted in glass-ceramics with a small amount of glassy phase retained in the structure. Peaks of cubic yttria-stabilized zirconia were found in all of the X-ray diffraction patterns. Other crystalline phases identified by X-ray diffraction analysis are listed in Table 5. They are consistent with those found in previous studies.<sup>2</sup> Yttrium disilicate ( $\text{Y}_2\text{Si}_2\text{O}_7$ ) crystallized from the glass in the form of two polymorphs  $\beta$  (JCPDS-22-1103) and  $\gamma$  (JCPDS-32-1448). Small traces of mullite ( $\text{Al}_6\text{Si}_2\text{O}_{13}$ ) were present in all X-ray diffraction patterns.

The  $\text{Al}_2\text{O}_3$  phase, expected because the existence

Table 4. Vickers hardness and density of zirconia-containing glasses

Composition	$\text{ZrO}_2$ content (wt%)	VH (GPa)	Density ( $\text{g cm}^{-3}$ )
3C	0	$7.96 \pm 0.46$	3.63
6	2	$7.89 \pm 0.20$	3.69
7	5	$8.09 \pm 0.18$	3.73
8	6	$8.65 \pm 0.22$	3.76
9	7	$8.73 \pm 0.21$	4.43
10	8	$8.42 \pm 0.53$	4.44

Table 5. X-ray powder diffraction analysis for composition 8 with the addition of 6 wt% of zirconia heat treated in nitrogen for 1 h

Crystallization temp. (°C)	Phase
950	Clear amorphous glass
1000	Clear amorphous glass
1050	Opaque amorphous glass
1100	$\gamma$ - $\text{Y}_2\text{Si}_2\text{O}_7$ , s; $\beta$ - $\text{Y}_2\text{Si}_2\text{O}_7$ , w; $\text{Al}_6\text{Si}_2\text{O}_{13}$ , vw;
1150	$\gamma$ - $\text{Y}_2\text{Si}_2\text{O}_7$ , s; $\beta$ - $\text{Y}_2\text{Si}_2\text{O}_7$ , w; $\text{Al}_6\text{Si}_2\text{O}_{13}$ , vw;
1200	$\gamma$ - $\text{Y}_2\text{Si}_2\text{O}_7$ , s; $\beta$ - $\text{Y}_2\text{Si}_2\text{O}_7$ , m; $\text{Al}_6\text{Si}_2\text{O}_{13}$ , vw;
1250	$\beta$ - $\text{Y}_2\text{Si}_2\text{O}_7$ , s; $\gamma$ - $\text{Y}_2\text{Si}_2\text{O}_7$ , w; $\text{Al}_6\text{Si}_2\text{O}_{13}$ , vw;
1300	$\beta$ - $\text{Y}_2\text{Si}_2\text{O}_7$ , s; $\gamma$ - $\text{Y}_2\text{Si}_2\text{O}_7$ , w; $\text{Y}_3\text{Al}_5\text{O}_{12}$ , vw; $\text{Al}_6\text{Si}_2\text{O}_{13}$ , vw; $\text{Al}_6\text{Si}_2\text{O}_{13}$ , vw
1350	$\beta$ - $\text{Y}_2\text{Si}_2\text{O}_7$ , s; $\gamma$ - $\text{Y}_2\text{Si}_2\text{O}_7$ , vw; $\text{Al}_6\text{Si}_2\text{O}_{13}$ , vw

s is strong, m is medium, w is weak and vw is very weak.

of the  $2 \text{ Y}_2\text{O}_3 \cdot 3 \text{ SiO}_2$  phase has been questioned, was detected neither by X-ray nor SEM analysis, which confirms results by Hyatt and Day.<sup>9</sup> A very small amount of YAG ( $\text{Y}_3\text{Al}_5\text{O}_{12}$ ) was identified after the 1300 and 1350°C treatments by X-ray analysis. It is important to emphasize that the specimens were heat-treated at the elevated temperatures for only 1 h and then quenched very rapidly. Therefore, equilibrium conditions were not reached and consequently some additional, probably intermediate, phases were observed. Although they could not be identified using JCPDS tables, the existence of such phases has been reported in earlier studies.<sup>2,3</sup> Dinger *et al.*<sup>18</sup> reported the existence of a low-temperature, impurity-stabilized  $\gamma$ -polymorph of  $\text{Y}_2\text{Si}_2\text{O}_7$ , that transforms to  $\alpha$ - $\text{Y}_2\text{Si}_2\text{O}_7$  upon heating at 1200°C and to  $\delta_1$  and  $\delta_2$  upon heating above 1200°C. Drummond<sup>3</sup> observed the formation of the  $\beta$ - $\text{Y}_2\text{Si}_2\text{O}_7$  polymorphs when adding zirconia as a nucleating agent. The crystallographic data for the compounds in the  $\text{Y}_2\text{O}_3$ - $\text{NSiO}_2$  system have been summarized recently by several investigators (see, e.g. Refs 30 and 31).

SEM investigations in this study revealed that the crystallization of the glass is probably governed by a number of mechanisms acting at different temperatures. The different types of phase transformation observed in the glass can be summarized as follows:

- (i) crystallization of  $\beta$ - $\text{Y}_2\text{Si}_2\text{O}_7$ ;
- (ii) crystallization of  $\gamma$ - $\text{Y}_2\text{Si}_2\text{O}_7$ ;
- (iii) crystallization of yttria stabilized  $\text{ZrO}_2$  ( $\text{Y-ZrO}_2$ );
- (iv) transformation of  $\gamma$ - $\text{Y}_2\text{Si}_2\text{O}_7$  to  $\beta$ - $\text{Y}_2\text{Si}_2\text{O}_7$ ;
- (v) transformation of a Y-Al-Si-rich phase to  $\beta$ - $\text{Y}_2\text{Si}_2\text{O}_7$ .

At 1100°C, the sample is almost fully crystallized, with only a small amount of retained glassy

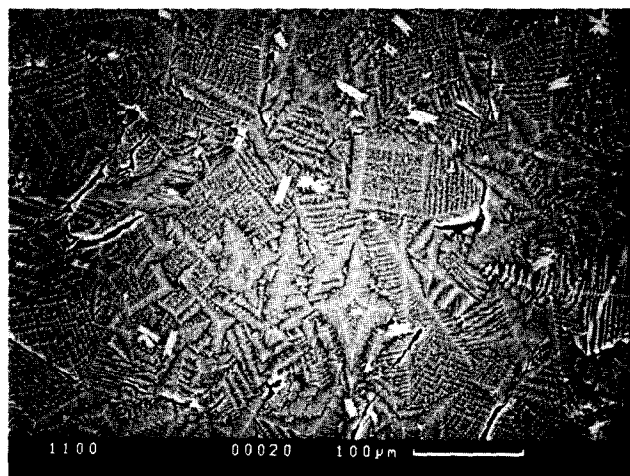


Fig. 5. Crystallization at 1100°C. (backscatter image — 200×).

phase (Fig. 5). The  $\gamma$ - $\text{Y}_2\text{Si}_2\text{O}_7$  is the dominant phase at this treatment temperature. At 1150 and 1200°C, a Y–Al–Si-rich phase appears in the microstructure and starts to transform to  $\beta$ - $\text{Y}_2\text{Si}_2\text{O}_7$  and probably mullite (Fig. 6). At 1300°C, the  $\beta$ - $\text{Y}_2\text{Si}_2\text{O}_7$  phase begins to dominate the microstructure (Fig. 7) and the  $\gamma$ - $\text{Y}_2\text{Si}_2\text{O}_7$  phase also starts to transform to the  $\beta$ - $\text{Y}_2\text{Si}_2\text{O}_7$  phase while the phase transformation of the Y–Al–Si-rich phase continues. At 1350°C, the dominant phase is  $\beta$ - $\text{Y}_2\text{Si}_2\text{O}_7$ . The microstructure begins to lose its dendritic appearance and the transformation of the  $\gamma$ - $\text{Y}_2\text{Si}_2\text{O}_7$  phase to the  $\beta$ - $\text{Y}_2\text{Si}_2\text{O}_7$  phase continues (Fig. 8).

The transformation of the  $\gamma$ - to the  $\alpha$ -polymorph was not observed. At higher temperatures the  $\gamma$ - $\text{Y}_2\text{Si}_2\text{O}_7$  polymorph starts to transform to the  $\beta$ - $\text{Y}_2\text{Si}_2\text{O}_7$  polymorph (stable at temperatures between 1225 and 1445°C in the binary  $\text{Y}_2\text{O}_3$ – $\text{SiO}_2$  system.<sup>3,10</sup>



Fig. 6. Y–Al–Si-rich phase at 1200°C with part of a  $\gamma$ - $\text{Y}_2\text{Si}_2\text{O}_7$  loose network and Y–ZrO<sub>2</sub> particles (backscatter image — 5000×).

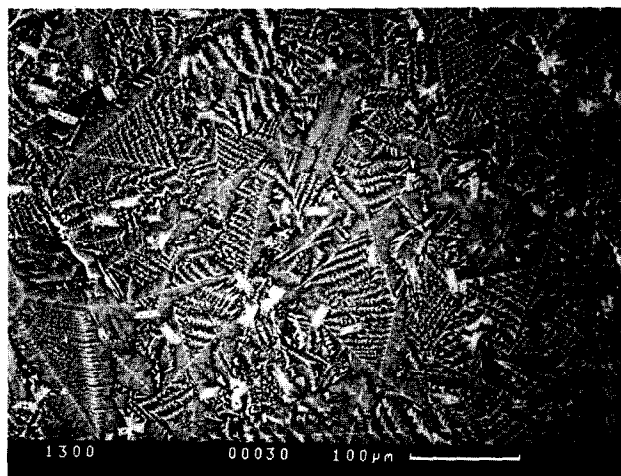


Fig. 7. Crystallization at 1300°C (backscatter image — 200×).

#### 4 Conclusions

Properties of yttria–alumina–silica compositions fired in nitrogen at 1600, 1650 and 1700°C have been assessed. The results are consistent with previous studies. ZrO<sub>2</sub> (6 wt%) can be dissolved in the investigated composition of the yttria–alumina–silica liquid at 1700°C. When larger amounts are added, a cubic crystalline phase of ‘yttria-stabilized zirconia’ with a composition of  $\text{Y}_{0.15}\text{Zr}_{0.85}\text{O}_{1.9}$  forms. The hardness and density of the glass increased slightly with addition of ZrO<sub>2</sub>.  $\gamma$ - $\text{Y}_2\text{Si}_2\text{O}_7$  (at temperatures <1300°C) and  $\beta$ - $\text{Y}_2\text{Si}_2\text{O}_7$  (at temperatures >1300°C) monoclinic phases formed during the crystallization. Very small amounts of mullite in all cases, and yttrium aluminium garnet at 1300 and 1350°C, were also observed. An unidentified intermediate phase rich in Y, Al and Si was observed to undergo a transformation at temperatures  $\geq 1200^\circ\text{C}$ , probably resulting in the formation of the  $\beta$ - $\text{Y}_2\text{Si}_2\text{O}_7$  phase.

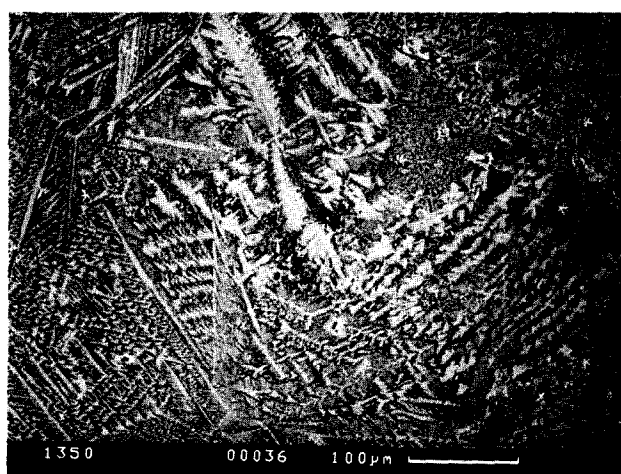


Fig. 8. Crystallization at 1350°C (backscatter image — 200×).

## References

1. Cinibulk, M. K. & Thomas, G., Grain-boundary-phase crystallization and strength of silicon nitride sintered with a YSiAlON glass. *J. Am. Ceram. Soc.*, **73**(6) (1990) 1606–12.
2. Arita, I. H., Wilkinson, D. S. & Purdy, G. R., Crystallization of Yttria–alumina–silica glasses. *J. Am. Ceram. Soc.*, **75**(12) (1992) 3315–20.
3. Drummond, C. H., III, Glass-formation and crystallization in high-temperature glass-ceramics and  $\text{Si}_3\text{N}_4$ . *J. Non-Cryst. Solids*, **123** (1990) 114–28.
4. Kleebe, H.-J., Cinibulk, M. K., Cannon, R. M. & Ruhle, M., Statistical analysis of the intergranular film thickness in silicon nitride ceramics. *J. Am. Ceram. Soc.*, **76**(8) (1993) 1969–77.
5. Clarke, D. R., On the equilibrium thickness of intergranular glass phases in ceramic materials. *J. Am. Ceram. Soc.*, **70**(1) (1987) 15–22.
6. Bondar, I. A. & Galakov, F. Y., Phase equilibria in the system  $\text{Y}_2\text{O}_3\text{--Al}_2\text{O}_3\text{--SiO}_2$ . *Izv. Akad. Nauk. SSSR Ser. Khim.*, **7** (1964) 1325–6.
7. Leng-Ward, G. & Lewis, M. H., Crystallization in Y–Si–Al–O–N glasses. *Mater. Sci. Engng.*, **71** (1985) 101–11.
8. Meara, C. O., Dunlop, G. L. & Pompe, R., Phase relationship in the system  $\text{Y}_2\text{O}_3\text{--Al}_2\text{O}_3\text{--SiO}_2$ . In *Proc. World Congress on High Tech Ceramics (6th CIMTEC)*, Milan, Italy, ed. P. Vincenzini. Elsevier Science Publishers, Amsterdam, 1986, pp. 265–70.
9. Hyatt, M. J. & Day, D. E., Glass properties in yttria–alumina–silica system. *J. Am. Ceram. Soc.*, **70**(10) (1987) C-283–7.
10. Drummond, C. H., III & Lee, W. E., Crystallization and characterization of  $\text{Y}_2\text{O}_3\text{--SiO}_2$  glasses. *Ceram. Engng. Sci. Proc.*, **9**(9–10) (1988) 1343–54.
11. Makishima, A., Tamura, Y. & Sakaino, T., Elastic moduli and refractive indices of aluminosilicate glasses containing  $\text{Y}_2\text{O}_3$ ,  $\text{La}_2\text{O}_3$  and  $\text{TiO}_2$ . *J. Am. Ceram. Soc.*, **61**(5–6) (1978) 247–9.
12. Sedych, T. S., Pustilnik, A. I. & Mikheikin, V. I., Refractive indices in the system  $\text{Y}_2\text{O}_3\text{--Al}_2\text{O}_3\text{--SiO}_2$  in the vitrification region. *Akad. Nauk SSSR, Neorg. Mater.*, **11**(6) (1975) 1153–4.
13. Loehman, R. E., Preparation and properties of yttrium–silicon–aluminum oxynitride glasses. *J. Am. Ceram. Soc.*, **62**(9–10) (1979) 491–4.
14. Loehman, R. E., Oxynitride glasses. *J. Non-Cryst. Solids*, **42** (1980) 433–46.
15. Loehman, R. E., Preparation and properties of oxynitride glasses. *J. Non-Cryst. Solids*, **56** (1983) 123–34.
16. Lewis, M. H., Crystallisation of grain boundary phases in silicon nitride and sialon ceramics. *Key Engng Mater.*, **89–91** (1994) 333–8. Trans Tech Publications, Switzerland.
17. Lewis, M. H., Bhatti, A. R., Lumby, R. J. & North, B., The microstructure of sintered Si–Al–O–N ceramics. *J. Mater. Sci.*, **15** (1980) 103–13.
18. Dinger, T. R., Rai, R. S. & Thomas, G., Crystallization behaviour of a glass in the  $\text{Y}_2\text{O}_3\text{--SiO}_2\text{--AlN}$  system. *J. Am. Ceram. Soc.*, **71**(4) (1988) 236–44.
19. Besson, J. L., Billieres, D., Rouxel, T., Goursat, P., Flynn, R. & Hampshire, S., Crystallization and properties of a Si–Y–Al–O–N glass-ceramic. *J. Am. Ceram. Soc.*, **76**(8) (1993) 2103–5.
20. O'Meara, C. & Dunlop, G. L., Formation, crystallization and oxidation of selected glasses in the Y–Si–Al–O–N system. *J. Eur. Ceram. Soc.*, **8** (1991) 161–70.
21. Ekström, T., Transient liquid phase sintering of silicon nitride. In *Proc. Int. Ceramic Conference Austceram 90*, Perth, Australia, eds P. J. Darragh and R. J. Stead. Trans. Tech. Publications, 1990, pp. 586–91.
22. Knutson-Wedel, E. M., Falk, L. K. L. & Ekström, T.,  $\text{Si}_3\text{N}_4$  ceramics formed by HIP using additions of  $\text{ZrO}_2$ . In *Ceramics Today–Tomorrow's Ceramics*. Elsevier Science Publishers B.V., 1991.
23. Knutson-Wedel, E. M., Falk, L. K. L. & Ekström, T.,  $\text{Si}_3\text{N}_4\text{--ZrO}_2$  Composites with small  $\text{Y}_2\text{O}_3$  and  $\text{Al}_2\text{O}_3$  additions prepared by HIP. *J. Mater. Sci.*, **26** (1991) 4331–40.
24. Knutson-Wedel, E. M., Falk, L. K. L. & Ekström, T., Microstructures and properties of  $\text{Si}_3\text{N}_4$  ceramics formed by HIP using different oxide additives. In *Proc. 11th Risø Int. Symp. on Metallurgy and Materials Science*, Denmark, 1990.
25. Knutson-Wedel, E. M., Falk, L. K. L. & Ekström, T., Pressureless-sintered  $\text{Si}_3\text{N}_4\text{--ZrO}_2$  composites with  $\text{Y}_2\text{O}_3$  and  $\text{Al}_2\text{O}_3$  additions. *J. Mater. Sci.*, **9** (1990) 823–6.
26. Zhao, J., Wang, L., Peng, G. & Wu, J. G., Effect of zirconia on the crystallization of grain boundary. *Proc. 4th Int. Symp. on Ceramic Materials and Components for Engines*, Gothenburg, Sweden, 1990.
27. Ding Yuquan, Ding Zishang & Jiang Zhonghua, Formation and properties of Y–Al–Si–O–N system in the grain boundaries of  $\text{Si}_3\text{N}_4$  ceramics. *J. Non-Cryst. Solids*, **112** (1989) 408–12.
28. Lazarev, A. N., *Vibrational Spectra and Structure of Silicates*. Plenum Press, New York, 1972.
29. Sato, R. K., Bolvin, J. & McMillan, P. F., Synthesis and characterization of a SiAlON glass. *J. Am. Ceram. Soc.*, **73**(8) (1990) 2494–7.
30. Lee, W. E., Drummond, C. H. III, Hilmas, G. E. & Kumar, S., Microstructural evolution in near-eutectic yttrium silicate compositions fabricated from a bulk melt and as an intergranular phase in silicon nitride. *J. Am. Ceram. Soc.*, **73**(12) (1990) 3575–9.
31. Kumar, S. & Drummond, C. H. III, Crystallization of various compositions in the  $\text{Y}_2\text{O}_3\text{--SiO}_2$  system. *J. Mater. Res.*, **7**(4) (1992).